

Active CO₂ reservoir management for sustainable geothermal energy extraction and reduced leakage

Thomas R. Elliot, Princeton University, Civil and Environmental Engineering, NJ, USA

Thomas A. Buscheck, Lawrence Livermore National Laboratory, Geochemical, Hydrological, and Environmental Sciences Group, Livermore, CA, USA

Michael Celia, Princeton University, Civil and Environmental Engineering, NJ, USA

Abstract: Subsurface storage space is gaining recognition as a commodity for industrial and energy recovery operations. Geologic carbon dioxide (CO₂) sequestration (GCS), wherein supercritical CO₂ is injected into subsurface storage space, is under broad development in sedimentary reservoirs – particularly for hydrocarbon production, which uses supercritical CO₂ as part of a carbon capture utilization and sequestration (CCUS) scheme. A novel CCUS operation is presented whereby we investigate the staged deployment of a coupled geothermal energy extraction (GEE)-GCS operation in geothermal sedimentary reservoirs that re-circulates extracted fluids. We identify sedimentary resources of the continental USA that have significant temperature at depths suitable for GCS. To predict the impact of a GEE-GCS operation, a reservoir-scale semi-analytical model is used to simulate brine and CO₂ migration through existing leakage pathways. With the goal of integrating GEE and GCS, a well-site design exercise is undertaken, where we develop an idealized configuration for CO₂ and brine production/reinjection wells. Results show potential geothermal sedimentary reservoirs suitable for GEE deployment exist in the continental USA; however the characteristics of each site should be investigated through a first stage GEE-operation to determine GCS capacity. Our active CO₂ reservoir management simulations demonstrate a decrease in injection and reservoir overpressures, a reduced migration of CO₂ within the reservoir during active injection/extraction, and a reduced risk of brine and CO₂ migration. With the use of the developed concentric-ring well pattern, we demonstrate the longevity of thermal productivity from an ideal GEE site, while providing sufficient CO₂ storage volume and trapping to act as a sequestration operation.

© 2013 Society of Chemical Industry and John Wiley & Sons, Ltd

Keywords: carbon sequestration; geothermal; CCUS; subsurface hydrology; carbon capture and utilization

Introduction

Geologic carbon dioxide (CO₂) sequestration (GCS), a process where supercritical CO₂ is injected into subsurface storage space, is a

specific utilization of sedimentary reservoirs that is under broad development.¹ If significant deployment of GCS in the continental United States (USA) were to occur, the operations would fall under US Environmental Protection Agency Underground Injection

Correspondence to: Thomas R. Elliot, Princeton University, CEE, 59 Olden St, Princeton, NJ 08544, USA. E-mail: elliot.thomas.r@gmail.com

Received August 25, 2012; revised November 11, 2012; accepted November 26, 2012

Published online at Wiley Online Library (wileyonlinelibrary.com). DOI: 10.1002/ghg.1328



Control (UIC) Class VI well regulations. The resulting large-scale CO₂ sequestration program would face a number of uncertainties and risks that would need to be addressed to satisfy UIC requirements. These include our limited ability to predict specific reservoir storage capacity² and injectivity,³ especially for virgin GCS reservoirs that do not benefit from knowledge gained from earlier oil or gas development. This limited ability for reliable prediction comes from the significant uncertainty in subsurface characteristics⁴ and lack of injection data for virgin GCS reservoirs. These uncertainties are seen as primary barriers to secure GCS deployment.⁵ Secondary barriers to deployment include low or non-existent economic incentives for operators and general issues of public acceptance, including not-in-my-back-yard attitudes and general skepticism of climate change.⁵

Overpressure (pressure in excess of ambient) can be the limiting factor for CO₂ injection rates and is also the main physical drive for potential brine migration and an important factor for CO₂ leakage. By utilizing an active CO₂ reservoir management (ACRM) approach, where resident brine is extracted from the injection reservoir and redistributed spatially, it is possible to modify/reduce the subsurface overpressure associated with large-scale injection operations.^{6,10} If the extracted brine has low enough salinity and can be treated with softeners and scale inhibitors,¹⁰ it can be used for industrial purposes such as (saline) cooling water or, if the brine composition is compatible, as make-up fluid for pressure support in neighboring reservoir operations such as hydraulically enhanced hydrocarbon production or for Enhanced Geothermal Systems (EGS).^{8,31} Depending on brine salinity, there is also the potential for desalination. If a sedimentary formation has sufficient thermal gradient, as well as appropriate depth, permeability, pore volume, and horizontal continuity, ACRM-enhanced GCS and geothermal energy extraction (GEE) can be conjunctively deployed.

A hot dry rock geothermal energy (EGS) concept utilizing CO₂ instead of water as the working fluid was first proposed by Brown⁴⁰ and would achieve geologic sequestration of CO₂ as an ancillary benefit. Pruess¹¹ followed up on this idea by evaluating thermophysical properties and performing reservoir simulations. Pruess¹¹ analyzed a five-spot pattern with four CO₂ injectors and a producer in the center, with 707-km spacing between the producer and injectors and found CO₂ to be superior to water in mining heat from hot

fractured rock, including a reduced parasitic power consumption to drive the fluid circulation system. This concept has been extended to GCS in saline, sedimentary formations,^{7,12,41} which they call a CO₂-plume geothermal (CPG) system to distinguish it from CO₂-enabled EGS in crystalline rock. Because it is targeted for large, porous, permeable sedimentary basins, CPG can result in significantly more CO₂ sequestration and more geothermal heat extraction than CO₂-based EGS in crystalline rock. As stated in their patent,¹³ CO₂ sequestration is a primary goal for CPG. Randolph and Saar^{7,12,41} have analyzed this approach for the same five-spot well configuration as analyzed by Pruess.¹¹ With respect to parasitic energy costs for driving the fluid circulation system, Randolph and Saar¹² found CO₂ to be more efficient than water and brine for low-to-moderate permeability ($k < 2 \times 10^{-14}$ to 2×10^{-13} m²).

Existing reservoir studies of GEE-GCS fall under two end-member approaches to CO₂ utilization. The first approach, discussed above, focuses on utilizing CO₂ as an efficient geothermal working fluid because of advantageous thermo-physical properties, namely the low viscosity of CO₂, which reduces parasitic power consumption of the working-fluid circulation system.^{7,12,13,41} By maximizing the heat-extraction benefit per ton of delivered (i.e. captured) CO₂, this approach can significantly improve the economics of CO₂ capture and sequestration. The second approach focuses on utilizing CO₂ injection as a means of providing pressure support for geothermal production wells.^{8,31} The goals of the second approach are to maximize permanent CO₂ storage, reduce overpressure-driven risks of induced seismicity and CO₂ and brine leakage, and, where feasible, to generate significant quantities of water as an ancillary benefit. Depending on how it is deployed, the second approach can also maximize the heat-extraction benefit per ton of delivered CO₂. The first approach attempts to limit brine production, while the second approach attempts to delay/limit CO₂ production. Both approaches share the trait of potentially enabling geothermal energy production in regions where water scarcity may otherwise hinder geothermal deployment.

In this paper we analyze a staged GEE-GCS scheme, which combines conventional brine-based GEE practice with the two end-member GEE-GCS approaches described above, and conduct a GIS survey of US sedimentary basins to illustrate its deployment potential. We discuss how this scheme can reduce

uncertainty about reservoir characteristics, provide direct thermal or electric energy production, and reduce the migration distances of resident brine and the sequestered CO₂.

Staged GEE-GCS deployment

The concept of GEE-GCS is relatively new, with most existing research specifically exploring CO₂ as a potentially advantageous working fluid for geothermal energy production.^{7,12,13,41} In such scenarios, captured CO₂ is used as the injection fluid in the geothermal operation. Herein we recommend enhancing and expanding this novel idea. Instead of using CO₂ as the sole working fluid, we recommend a flexible, staged approach that can adapt to site-specific conditions and factors. Factors include fluctuating aspects of resource supply and infrastructure, such as proximity to CO₂ sources, the cost of CO₂, and the availability of local water resources, as well as geologic conditions discovered during the reservoir characterization and early energy production stages. Subsurface characterization for a typical GCS program, prior to injection of CO₂, is costly. Remote sensing and pilot wellbores for injection tests are some of the tools required to parameterize the reservoir, which would incur up-front costs without a guaranteed return on investment. To reduce this operational exposure, we suggest that a geothermal plant using brine as a working fluid be deployed as the initial stage to identify appropriate reservoir characteristics. Tracer experiments and push-pull well tests can be conducted to identify the ideal GCS injection intervals (along the vertical direction) within a reservoir, and the overpressure would be reduced due to brine loss associated with GEE operations (e.g. evaporative loss and formation leak-off) to prepare a reservoir for GCS.

Once characterization is sufficient to reduce operational exposure and satisfy public acceptance surrounding GCS safety, the second stage can commence with CO₂ injection providing pressure support to maintain productivity of geothermal wells, while the ongoing loss of brine provides pressure relief and improved injectivity for the GCS program. The third stage of our recommended implementation is a hybrid brine-/CO₂-based GEE-GCS stage, which starts when CO₂ breakthrough occurs at an extractor well. Co-production of brine and supercritical CO₂ can generate a corrosive environment for the wellbore casing and surface equipment, which will require

careful study, along with the development of operational practices to mitigate potentially deleterious consequences. The injection of CO₂-enriched brine has the potential of creating reactive conditions within the reservoir and caprock, possibly affecting the integrity of well cement sheaths. These issues, which are beyond the scope of this paper, should be evaluated in future studies. To further reduce investment risk for operators, the GEE program can either provide regional heating options in the case of low thermal-yield basins, or a direct base-load energy supplement in the case of a high thermal-yield basin, through a hybrid brine-CO₂ geothermal plant.

As originally proposed by Buscheck,⁸ a key objective for GEE-GCS was for brine extraction to provide pressure relief for CO₂ injection, thereby increasing CO₂ storage capacity and efficiency while reducing the risks associated with overpressure. From the geothermal energy production perspective, a key objective for CO₂ injection was to provide pressure support, thereby increasing the productivity of brine extraction wells, rather than utilizing CO₂ as a working fluid for heat extraction. For those reasons, it was thought to be important to delay CO₂ breakthrough at the brine extraction wells in order to maximize their useful lifetime.^{9,10} Hence, those studies considered relatively large injector/extractor spacing. Early research on GEE-GCS has investigated CO₂ as a working fluid, primarily due to its low viscosity, compared to that of brine.^{7,12,41} To maximize the heat extraction per ton of delivered CO₂, those GEE-GCS studies have focused on small injector/extractor well spacing in order to promote early CO₂ breakthrough and recirculation.^{7,12,41} In order to efficiently use CO₂ as a working fluid, the first approach attempts to limit the amount of unrecovered CO₂ (permanent storage). It is worth noting that the previous work on GEE-GCS that emphasized CO₂ as a working fluid has not addressed the management of co-produced brine or considered its potential use as a working fluid.^{7,11,12,41} For the GEE-GCS cases presented later, we applied an injector/extractor spacing (1.38 km) that is a factor of two greater than that used in the 0.707-km well-spacing, 5-spot case analyzed by Randolph and Saar.⁷ As discussed later, the area between the CO₂ injectors and producers in our model is 15.7 km², or 1.96 km² per injector, which is twice the area per injector used in that study.⁷ Although, as discussed below, we achieved relatively early CO₂ breakthrough, we were never able to eliminate the co-production of brine,

even when the simulations were extended to a 1000-year continuous injection period. Therefore, the issue of brine management is likely to be important for reservoir operations, whether or not brine is considered as a candidate working fluid.

Reservoir issues requiring evaluation in an integrated GEE-GCS system include: (i) reservoir capacity and caprock seal integrity, (ii) well spacing and injection volume as related to CO₂ breakthrough and thermal drawdown, (iii) the geothermal heat flux in the sedimentary basin, and (iv) multi-fluid wellbore hydraulics. Other factors requiring evaluation include capital and operation and maintenance costs for (i) multiple injection and extraction wells, (ii) the network of pipelines, and (iii) the geothermal power plant facilities, as well as the nominal payout on the produced geothermal energy. Because the surface facilities will cover a wide area, implementation planning will need to address potential land-use conflicts in populated areas. In this paper we will address the first three reservoir issues, while leaving wellbore hydraulics and economic analyses for later studies.

Ideal characteristics of an integrated system

The characteristics of a reservoir that make it suitable for GCS are similar to those for ideal GEE reservoirs, namely that a formation (saline aquifer) have sufficient permeability, porosity, thickness, and horizontal continuity. GCS capacity increases with net brine removal (extraction minus reinjection) from the storage aquifer, which can be enabled by beneficial utilization/consumption of extracted brine for either fresh water generation via desalination technologies such as reverse osmosis (RO), or for use as saline cooling water. Beneficial brine consumption is favored by lower salinity, with current RO technology being capable of treating up to 85 000 mg/l TDS (total dissolved solids),^{10,14} while optimal GEE reservoirs should have a strong heat flux.¹⁵ The shared optimal traits would facilitate injection, migration, and storage of large fluid volumes, be it single-phase flow (brine for the first stage of GEE) or multi-phase flow (for GCS), with the added requirement of economically useful heat flux (and temperature). An active GEE program within a GCS reservoir would influence the migration of buoyant CO₂, which can be manipulated in a beneficial manner (e.g. to avoid interference with neighboring subsurface activities).¹⁰ Furthermore, CO₂

migration can be manipulated for the purpose of either delayed breakthrough, which would maximize pore-space utilization for GCS, or accelerated breakthrough at an extraction well, which would maximize utilization of CO₂ as a working fluid for GEE.^{9,10} For these reasons, it would be advantageous to (i) identify baffles or lower permeability regions in the structure of a reservoir that may force migrating CO₂ to occupy more of the vertical extent (i.e. be more cylindrical or piston-like),¹⁷ and (ii) design the injection-extraction well patterns and flow rates to optimize injection with formation characteristics for minimized risk of extraction-well CO₂ breakthrough, and to maximize the pore-space utilization of a given resource. Because the process of identifying the 3D reservoir structure will continue during well-field operations, optimization of the injection-extraction scheme will occur iteratively with ongoing reservoir characterization activities.

A similar requirement for an overlying (caprock) sealing unit exists for both GCS and GEE reservoirs, where a thick and continuous non-reactive (non-calcareous in the case of GCS) low permeability formation would be ideal.¹⁸ For CO₂ sequestration the sealing unit is needed to retain the buoyant injected fluid, whereas the geothermal operation would need an overlying barrier to prevent the drawdown of unwanted cool-formation waters into the brine production zone.

Operations engineering: methodology

In this study we conducted a GIS-based geothermal survey of US sedimentary basins, restricted to areas with a sediment depth suitable for GCS, and subsequently correlated geothermal gradient and depth of sedimentary formation data. One area identified by the survey was selected as a case-study site, for which formation injectivity and reservoir CO₂ storage capacity were acquired from literature sources. The semi-analytical computational model called estimating leakage semi-analytically (ELSA)¹⁹ was used to determine impact of ACRM and well-site design on reservoir pressure, CO₂ and brine migration out of the injection aquifer, and geothermal working fluid potential for GEE. To better understand the potential benefits and challenges of GEE-GCS deployment, without consideration of discrete leakage pathways, as are addressed in the ELSA model analyses, we construct a generic well-site model consisting of three concentric rings of wells, including an inner ring of

fluid (brine and CO₂) extraction wells, a middle ring of CO₂ injection wells, and an outer ring of brine reinjection wells. A case is also considered where the outer ring of eight vertical brine injectors is replaced by a square pattern of four horizontal brine injectors. The simulation was run using Lawrence Livermore National Laboratory's NUFT code²⁰ to capture detailed thermal and pressure responses as well as multi-phase, multi-component mass and heat balances in the near-well environment. The generic well-site model is not intended to represent a specific site; rather, it is used to represent a range of potential reservoir settings in sedimentary basins; hence, four different formation temperature cases are considered.

GIS survey

ESRI ArcMap™ version 10.2 was used to register the NATCARB saline reservoir database²¹ to a continental U.S. sediment thickness map,²² and subsequently resolve sediment depths greater than 1 km (note: 800 m is suitable for a 1045 kg/m³ brine hydrostatic

gradient to keep CO₂ in a supercritical state, but the authors felt that a 200 m 'buffer' would be a pertinent conservative assumption that is consistent with a 1 km depth regulation in Canada and Europe). This new base map, shown in Fig. 1, was used to identify storage sites, as reported in NATCARB, and calculate depth-dependent thermal properties for our modeling work.

Thermal flux, or potential temperature of target formations, was calculated for various sedimentary formations in the continental U.S. using depth-temperature maps,²³ in concert with surface temperature and heat flux maps. The temperature at depth was calculated through application of earth material heat-flux equations and correlated to reported bottom-hole temperatures, specifically Appendix Case A of Blackwell *et al.*²⁴ We calculated values for 2.25 km and 4.75 km to correspond to the generic well-site model section, however we only present the 2.25 km depth and the temperature at the crystalline basement in Fig. 2. We calculate temperature at depth using the heat flux contribution of surface temperature, radioactive

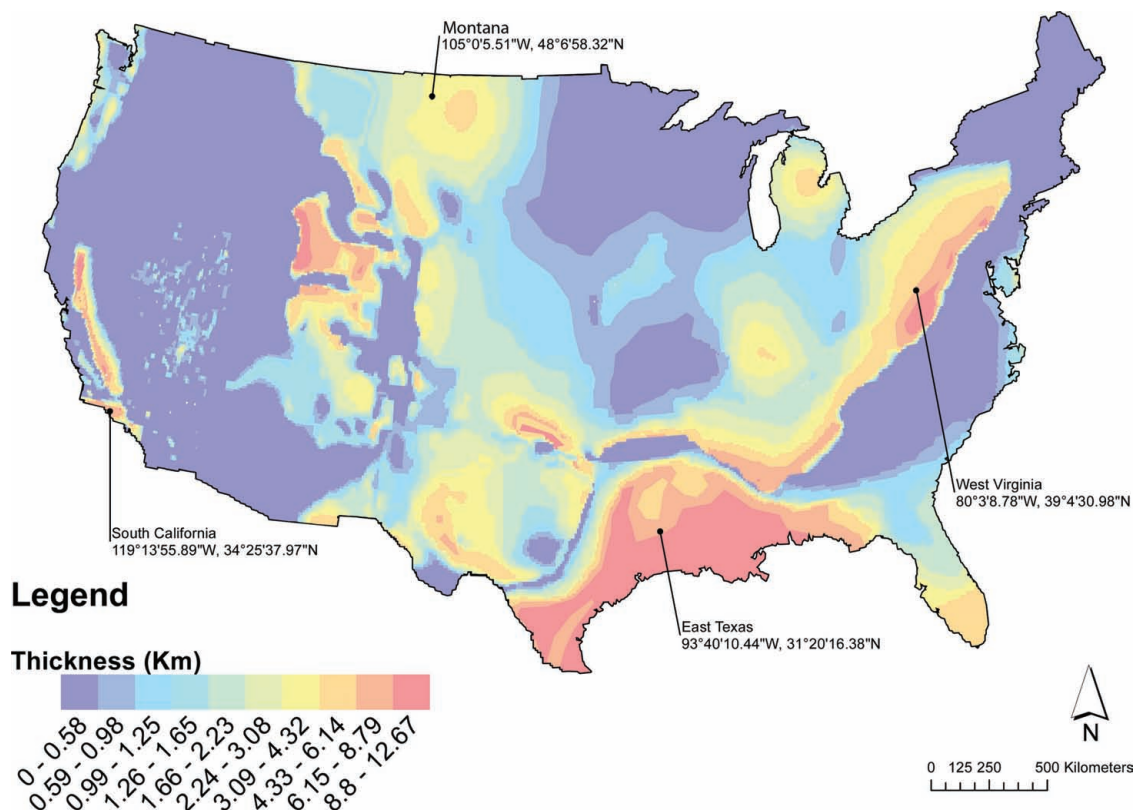


Figure 1. Thickness of sedimentary deposits, consolidated or otherwise, of the continental United States. Accumulation of deep sedimentary rocks correspond with clastic wedges (east and southern coasts), inland seas and major drainage basins (north-central USA and southern coast), and basins created during orogeny and subsequent weathering (west-coast).

Table 1(a). Hydrologic parameter values for the basin scale sequestration simulation and temperature at depth calculation.

| Parameter | Value | Parameter | Value |
|--|---|--|--|
| Material Properties | | | |
| Injection Aquifer thickness [m] | 250 | Overlying Aquifer thickness [m] | 50 |
| Injection Aquifer permeability [m ²] | 1.00 × 10 ⁻¹³ | Overlying Aquifer permeability [m ²] | 1.00 × 10 ⁻¹³ |
| Injection Aquifer porosity [L ³ /L ³] | 0.12 | Overlying Aquifer porosity [L ³ /L ³] | 0.12 |
| Sedimentary thermal conductivity [W/m/K] | 2.0 | Sedimentary radioactive heat generation [μW/m ³] | 1.0 |
| Igneous (basement) thermal conductivity [W/m/K] | 2.7 | Igneous radioactive heat generation [μW/m ³] | Spatially variable |
| Fluid Properties | | | |
| Residual Brine Saturation [V _r /V ₀] | 0.30 | CO ₂ Density [kg/m ³], in the injection/overlying aquifer | 446.06/456.84 |
| Relative Permeability of CO ₂ at residual brine saturation [m ² /m ² ₀] | 0.50 | CO ₂ Viscosity [Pa·s], in the injection/overlying aquifer | 3.89 × 10 ⁻⁵ /3.98 × 10 ⁻⁵ |
| Brine Compressibility [Pa ⁻¹] | 4.5 × 10 ⁻¹⁰ | Brine Density [kg/m ³], in the injection/overlying aquifer | 1035/1041 |
| Permeability of leaky wells [m ²], min/average/max | 10 ⁻¹⁸ /10 ⁻¹⁴ /10 ⁻¹⁰ | Brine Viscosity [Pa·s], in the injection/overlying aquifer | 6.56 × 10 ⁻⁴ /3.82 × 10 ⁻⁴ |

Table 1(b). Hydrologic and thermal parameter values used in the generic well-site model study.

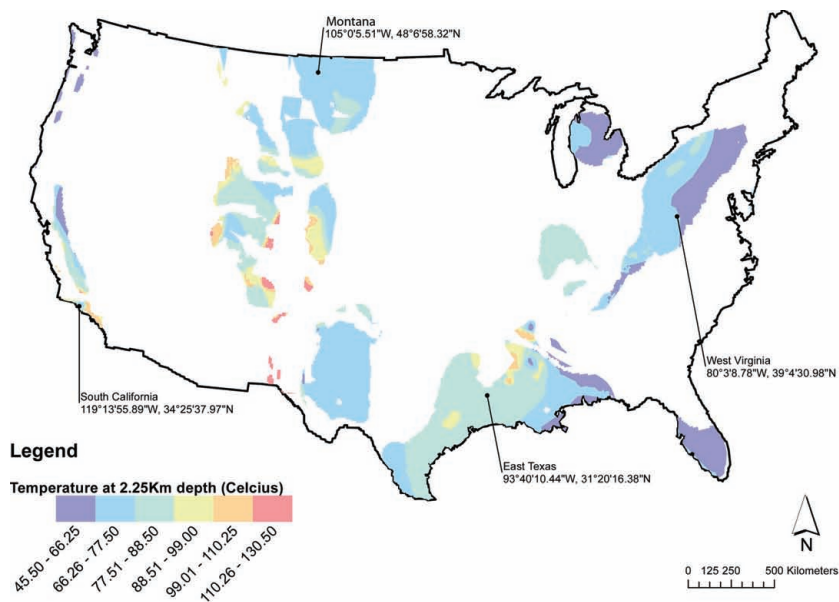
| Property | Aquifer | Sealing units |
|--|-------------------------|-------------------------|
| Horizontal and vertical permeability [m ²] | 1.0 × 10 ⁻¹³ | 1.0 × 10 ⁻¹⁸ |
| Pore compressibility [Pa ⁻¹] | 4.5 × 10 ⁻¹⁰ | 4.5 × 10 ⁻¹⁰ |
| Porosity [L ³ /L ³] | 0.12 | 0.12 |
| van Genuchten (1980) <i>m</i> | 0.46 | 0.46 |
| van Genuchten <i>a</i> [Pa ⁻¹] | 5.1 × 10 ⁻⁵ | 5.1 × 10 ⁻⁵ |
| Residual supercritical CO ₂ saturation | 0.05 | 0.05 |
| Residual water saturation | 0.30 | 0.30 |
| Thermal conductivity [W/m/K] | 2.0 | 2.0 |

decay within sedimentary material, and the crystalline basement/mantle, the rock material properties are shown in Table 1(a), and land surface temperature data is gathered from Wan.²⁵ To verify the calculations used in this article we compared the temperature values with depth-temperature maps²³ at various locations indicated in Fig. 2, and summarized in Table 2.

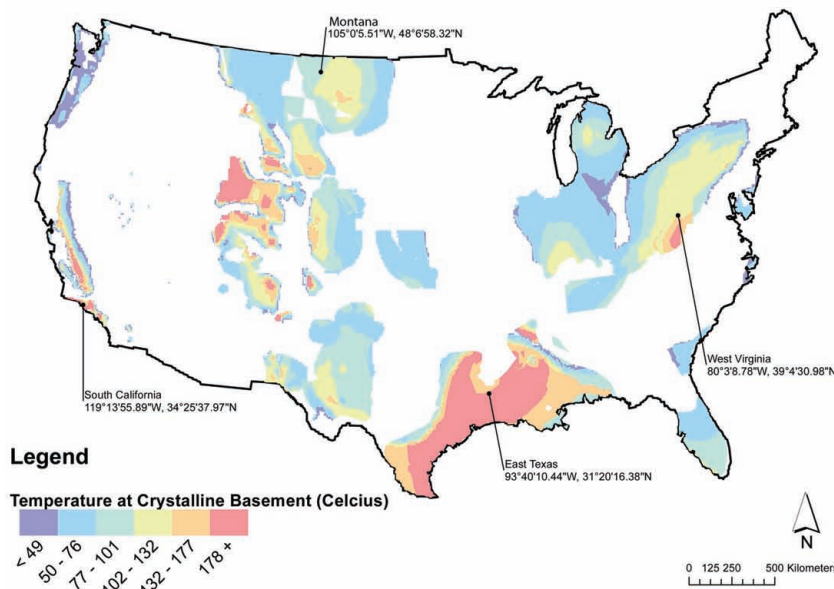
Basin-scale semi-analytic model

Modeling of pressure and fluid migration at a basin scale was conducted using Princeton University's

ELSA code,^{19,26} for the three-concentric ring, 24-spot, well-site design described in the next section. The well-site design is identical for the basin-scale and well-site models, except for the dimensionally reduced aspect of ELSA wherein the thickness dimension (i.e. CO₂ plume height assuming a sharp interface) is reconstructed from the semi-analytic equations. The Ellenberger formation in East-Central Texas, indicated in Fig. 1, was used as a proxy reservoir to provide formation and brine characteristics, as well as existing well locations within a 50 × 50 km domain. Reservoir parameters, other than those set forth by the generic well-site model presented later in this paper, were adopted from Chadwick²⁷ and are summarized in Table 1. Of note is the use of an open-flow *lateral* boundary for the reservoir-scale simulation, as opposed to the no-flow condition (representing a semi-closed reservoir) used for the generic well-site model. The open-flow boundary condition allows resident brine to be displaced laterally out of the model domain with no resulting overpressure whereas the semi-closed condition forces more vertical displacement of the brine through the impermeable caprock, which increases overpressure. As discussed later, the large basin area used in the generic well-site model renders the influence of the different lateral boundary conditions



(a)



(b)

Figure 2. (a) Temperature at 2.25 km depth, restricted to areas of the continental United States that has 2.25 km or more of sedimentary rock. (b) Temperature at the crystalline basement of the continental USA, with corresponding depths shown in Fig. 1. Four reference points are also indicated, which generally correlate to temperature findings of existing research, as shown in Table 2.

to be minor. The 35 existing wells were geospatially and depth-correlated from data gathered by the Texas Railroad Commission.²⁸ These wells were randomly assigned an effective vertical permeability value for

the aquitard section that each well passes through, thereby connecting super-positioned reservoir layers in the ELSA model. The permeability values were assigned from a normal Gaussian distribution

centered on 10^{-12} m² with a unit standard deviation.²⁹ A total of 15 million tonnes (MT) of CO₂ was injected per annum, distributed across all eight of the injection wells at a fixed flow rate for a period of 50 years. For the generic well-site model CO₂ injection is ramped from 15 to 30 MT per annum during the first 20 years. This is the quantity of CO₂ generated by 1.9 to 3.8 GWe of coal-fired power plants. The rationale for this assumption is that sites with formation temperatures favorable for GEE-GCS deployment will be much less prevalent than sites suitable for GCS deployment in general. Thus, it would be attractive to utilize such sites for sequestering CO₂ from multiple coal power plants, rather than just a single coal power plant.

Generic well-site model of a concentric, three-ring, well pattern

For a more detailed well-site model, we used the NUFT (non-isothermal unsaturated-saturated flow and transport) code, which simulates multi-phase heat and mass flow and reactive transport in variably saturated porous media.²⁰ We used a 3D model with quarter symmetry to represent a 250-m-thick storage aquifer, similar to that modeled by Zhou *et al.*³⁰ and Buscheck *et al.*^{9,10,31} Details of the aquifer properties and conditions (Table 1(b)) are found in Buscheck *et al.*³² The bottom of the storage aquifer is located either 2.5 or 5.0 km below the ground surface, with ambient pressures of 25 and 50 MPa, bounded by thick, relatively impermeable (10^{-18} m²) (caprock and bedrock) sealing units, which comprise the entire over- and under-burden. This choice is based on previous work, which showed that sealing-unit

thickness does not influence either overpressure or CO₂ migration in the storage aquifer when the sealing units are at least 50 m in thickness.¹⁰ Water density in the model is determined by the ASME steam tables, assuming pure water, rather than brine.³³ As has been done by Spycher and Pruess,³⁷ we will address the influence of total dissolved solids (TDS) of formation brine in future GEE-GCS studies. Two-phase flow of CO₂ and water was simulated with the density and compressibility of supercritical CO₂ determined by the Span and Wagner³⁴ correlation and viscosity determined by the Fenghour *et al.*³⁵ correlation. The outer boundaries have a no-flow condition to represent a semi-closed reservoir with an effective area of 31416 km², which is quite large and similar in size to the Illinois basin (~40,000 km²).³⁹ Because for this example there is only one GCS operation within a relatively large basin, pressure response is similar to that which would occur in an open system. The lower boundary, 1 km below the bottom of the reservoir, has a no-flow condition and a specific geothermal heat flux of either 75 or 100 mW/m². We used a single value of thermal conductivity of 2.0 W/m °C throughout the model domain, resulting in thermal gradients of 37.5 and 50 °C/km and temperatures of 104.0, 133.7, 197.8, and 258.7 °C, averaged over the vertical extent of the reservoir (Table 3).

We modeled a symmetrical 24-spot well pattern, consisting of three concentric rings of vertical wells, including an inner ring of 8 extractors (producers), each located 2 km from the center, a middle ring of 8 CO₂ injectors, 3 km from the center, and an outer ring of 8 brine injectors, 5 km from the center. The middle ring of CO₂ injectors are rotated 45 degrees relative to the inner ring of extractors in order to

Table 2. Correlation of temperature calculated in this article and borehole-correlated min/max temperature at depth²³ for the regions indicated in Figs 1 and 2. The selected Wyoming site did not have sedimentary deposits at depths of 4 km or greater, and therefore we do not report on those values.

| Location | 2 km [°C] | min/max | 3 km [°C] | min/max | 4 km [°C] | min/max | 5 km [°C] | min/max |
|---------------|-----------|----------|-----------|-----------|-----------|-----------|-----------|-----------|
| SW California | 71.5 | 50 / 75 | 93.75 | 75 / 100 | 114.0 | 100 / 125 | 132.25 | 125 / 150 |
| North Texas | 76.5 | 75 / 100 | 98.75 | 100 / 125 | 119.0 | 125 / 150 | 137.25 | 175 / 200 |
| West Virginia | 69.5 | 50 / 75 | 91.75 | 75 / 100 | 112.0 | 100 / 125 | 130.25 | 100 / 125 |
| Wyoming | 68.5 | 75 / 100 | 90.75 | 100 / 125 | - | - | - | - |

Table 3. Summary of results for the cases considered in the generic well-site model study.

| Geothermal heat flux [mW/m ²] | Reservoir bottom depth [km] | CO ₂ injection temperature [°C] | Initial extraction temperature [°C] | Initial heat extraction rate [MWt] | Time to 50% CO ₂ cut [years] | Temperature decline at 100 years [°C] |
|---|-----------------------------|--|-------------------------------------|------------------------------------|---|---------------------------------------|
| 75 | 2.5 | 16 | 104.0 | 434.4 | 13.6 | 8.6 |
| 75 | 2.5 | 47 | 104.0 | 434.4 | 13.6 | 7.2 |
| 100 | 2.5 | 16 | 133.7 | 553.8 | 15.8 | 10.5 |
| 100 | 2.5 | 51 | 133.7 | 553.8 | 15.8 | 8.7 |
| 75 | 5 | 16 | 197.8 | 824.0 | 19.4 | 7.8 |
| 75 | 5 | 47 | 197.8 | 824.0 | 19.4 | 7.0 |
| 100 | 5 | 16 | 258.7 | 1076.2 | 20.8 | 9.1 |
| 100 | 5 | 51 | 258.7 | 1076.2 | 20.8 | 7.9 |

increase the spacing between the CO₂ injectors and extractors from 1.0 to 1.38 km. The area between the CO₂ injectors and producers is 15.7 km², or 1.96 km² per injector, which is twice the area per injector used in previous studies.^{7,11–13} Because all of the extracted brine is re-injected in the outer ring of wells, this constrains the injected CO₂ to largely reside between the middle and inner rings of wells. CO₂ injection and fluid (brine plus CO₂) extraction (production) occurs over the entire vertical extent of the reservoir. In addition to pressure management reasons discussed below, this three-ring well pattern is motivated by the need to centralize fluid production and thereby minimize the distances that hot fluids will be conveyed to the geothermal plant.

Because brine extraction is assumed to be limited by the capacity of submersible pumps, a fixed rate of 120 kg/s is applied to each of the eight extractors, for a total fluid extraction rate of 960 kg/s. Note that when fluid extraction becomes primarily CO₂ it would be possible to increase the extraction rate above 120 kg/s due to the thermosyphon effect; however, for this study we fixed the fluid extraction rate. All extracted fluid is re-injected, with extracted brine injected in the outer ring of eight wells and extracted CO₂ injected in the middle ring of eight wells. Brine injection occurs in the upper half of the reservoir, which both counteracts the buoyant upward migration of the CO₂ plume and drives CO₂ toward the producers, thereby reducing the CO₂ breakthrough time. A second case was run where the outer ring of 8 vertical brine injectors is replaced by four horizontal brine injectors, located at the top of the reservoir to counteract buoyant CO₂ migration. The motivation

for using horizontal brine injectors is to spread brine injection, thereby reducing maximum overpressure.

A benefit of injecting all of the produced brine is to provide pressure support for the production wells. Without the pressure support from brine injection, bottom-hole pressures at the producers would drop well below hydrostatic, making it more difficult to maintain a production rate of 120 kg/s per well. Initially, fluid extraction is 100% brine, with the brine 'cut' (i.e., fraction) decreasing after CO₂ breakthrough. Because the brine reinjection rate declines along with the extracted brine cut, we were able to linearly ramp up the CO₂ injection rate from an initial rate of 60 kg/s per well to 120 kg/s at 20 years; thereafter it is fixed at 120 kg/s, for a total injection rate of 960 kg/s (30 MT per annum). CO₂ is injected at a fluid enthalpy corresponding to 16.0 °C at injection conditions, approximating typical average annual surface temperatures. This value of CO₂ injection temperature, which does not account for temperature rise occurring down the borehole resulting from the Joule-Thomson effect,³⁸ was chosen because it is conservative with respect to thermal drawdown. We also considered cases with a higher CO₂ injection temperature to examine the influence of that parameter. Extracted brine is re-injected at a fluid enthalpy corresponding to 16.0 °C at injection conditions, which is also conservative with respect to thermal drawdown.

Results and discussion

Geospatial survey results

The thickness (Fig. 1) and temperature (Fig. 2 for 2.25 km depth and crystalline basement) distributions

of sedimentary geologic formations used in this study are consistent with previous studies on the respective topics,¹¹ wherein the calculated thermal values (Table 2) generally correlate at various depths and locations indicated in Fig. 2. The minor deviations in the calculated temperature values of high-temperature reservoirs from measured values reported in other works (Table 2: Wyoming, East Texas) were most likely the result of several assumptions. The first is the use of a single value of thermal conductivity, which does not reflect the variable composition of sedimentary formations. The second is neglecting any mantle contribution to thermal accumulation, which is an effect that can be significant in regions where both crustal thinning²⁴ and mantle temperature anomalies at the Moho-interface²² can result in a non-linear temperature-depth relationship. There is less than 4 km of sediment for a geothermal hot spot in Wyoming, to which we limited our calculation of temperature for the purpose of GEE-GCS.

The distribution of low to moderate thermal values at 2.25 km depth, inclusive of temperatures over 125 °C, in sedimentary basins of the continental USA is restricted to prehistoric intra-continental seas in proximity to a historic volcanic sites and clastic-wedge accumulations at subduction/collision zones of accretion belts (Fig. 2). The only moderate thermal zone, at a calculated temperature of 60.75 °C, outside of this pattern is the lower peninsula of the state of Florida, which displays a homogeneous temperature distribution.

ELSA model results

Semi-analytical modeling of a 50 x 50 km domain with 35 pre-existing wells as potential sites of leakage using the injection well sight design, distributed as shown in Fig. 3, resulted in no predicted CO₂ leakage when the ACRM strategy is employed. Furthermore, the brine extraction and reinjection rate of the concentric, three-ring, well pattern induces a pressure gradient outside of the CO₂ plume, due to the exterior ring of brine reinjection wells, resulting in a pressure barrier to CO₂ migration. The impact of this three-ring well pattern on the reservoir scale is two-fold. Primarily, this ACRM strategy prevents CO₂ migration out of the injection aquifer – the efficacy of which can be modified through process optimization of extraction/reinjection rates, which would be coupled to operational targets for the CO₂ injection pressure. Process optimization can include beneficial brine

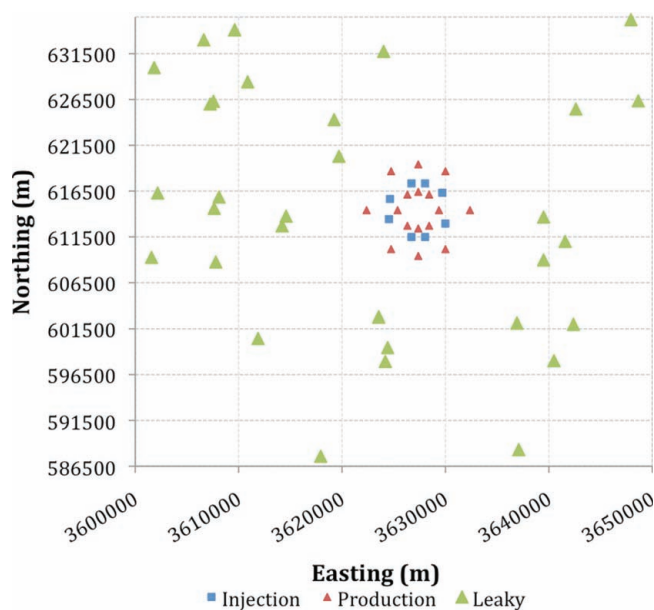


Figure 3. Spatial distribution of wells penetrating to the Ellenberger formation at the selected well site. This aerial view is used in the ELSA reservoir scale model to predict brine and CO₂ leakage through existing 'leaky' wells from a 24-well-site-design of ACRM GEE-GCS operation. The model employed is a three-layer geology (two aquifers, separated by an aquitard) with no-flow boundaries top and bottom, and pressure-boundary at the lateral extent of the 50 x 50 km domain.

consumption, wherein the brine reinjection rate is less than the brine extraction rate. Inherent evaporative brine loss in industrial processing will also cause the brine reinjection rate to be less than the extraction rate. The second impact of this ACRM strategy at reservoir scale is reduced overpressure for the middle ring of CO₂ injectors, which manifests as a power-law pressure decrease with increasing distance from the injector wells, when the inner-ring extractors draw brine away from the CO₂ injection wells. The field-scale ELSA model of pressure and CO₂ migration does indicate that nearly 0.8 MT of brine migrates out of the injection formation for a 50-year injection period, most of which passes through the lateral open boundary, with only a small fraction (~100 T) migrating vertically through leaky wells. This small volume of fluids displaced through leakage pathways is an added value for ACRM in conjunction with GCS, where a prevention effort on suspect wells or optimized injection would ensure that the GCS adheres to EPA UIC regulations prohibiting migration of formation fluids to overlying potable water aquifers.

Generic well-site model results

Figure 4 shows overpressure, brine saturation, and temperature simulated by the generic well-site model for the medium-high-temperature 24-spot, three-ring well-pattern case, the characteristics of which are presented in Table 1(b). The inner ring of extractors (producers) relieves overpressure at the CO₂ injectors. This well pattern effectively moves the region of greatest overpressure from the CO₂ injectors to the

outer ring of brine re-injectors (Figs 4(a) and 5), far removed from the CO₂ plume (Figs 4(b) and 4(c)). This approach reduces the risk of pressure-driven CO₂ leakage and constrains lateral migration. Because overpressure is dissipated over a much wider area than would have occurred without pressure management, via brine extraction, conveyance, and reinjection, the magnitude of overpressure is reduced. Because the injection of relatively cool CO₂ and brine

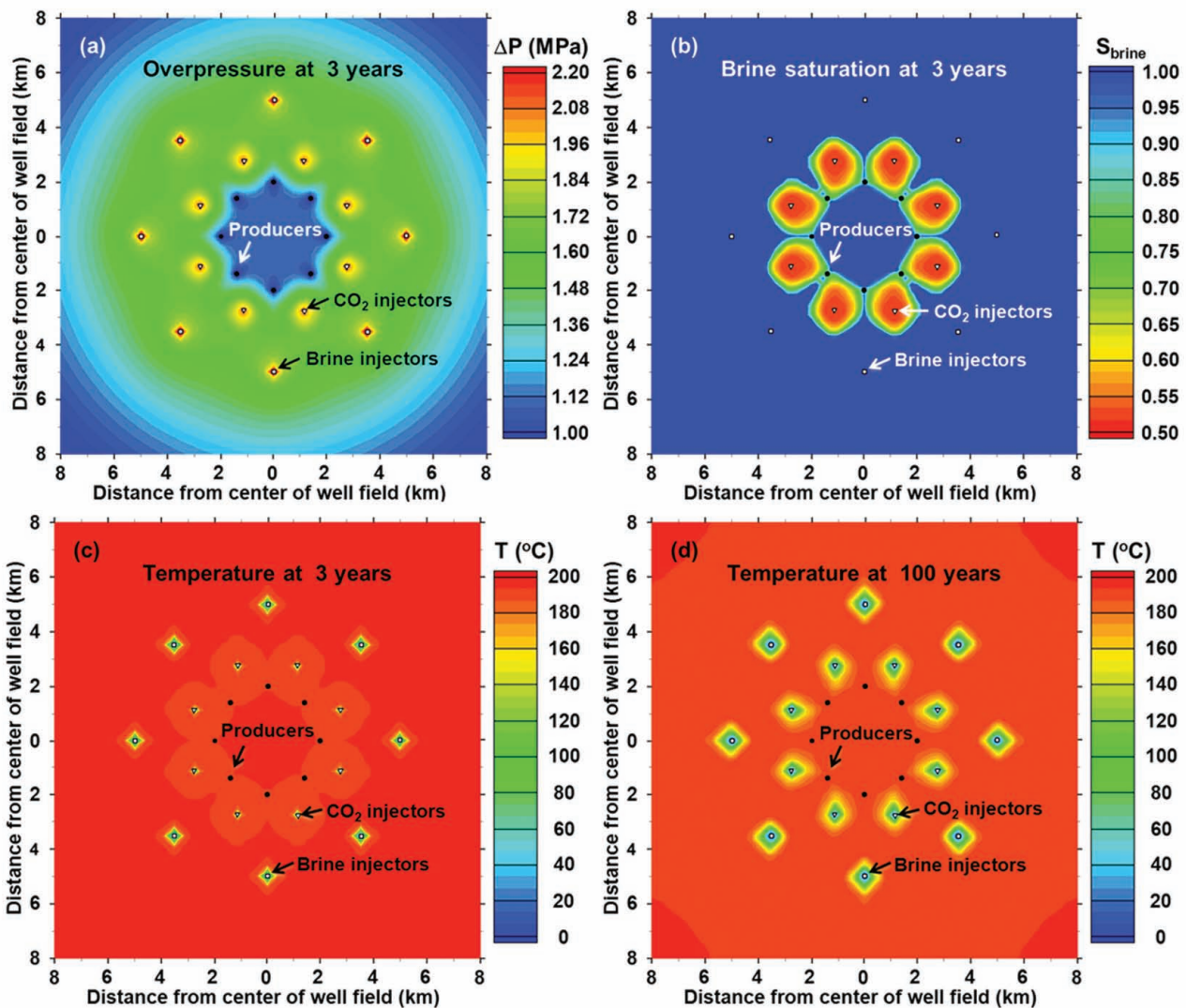


Figure 4. Overpressure, brine saturation, and temperature distributions are plotted at the indicated times for a symmetrical 24-spot, three-ring pattern of vertical wells, including an inner ring of eight extractors (producers), 2 km from the center, a middle ring of eight CO₂ injectors, 3 km from the center, and eight brine injection wells, 5 km from the center. A fixed fluid extraction rate of 960 kg/s is maintained, while the CO₂ injection rate is ramped from 480 to 960 kg/s from 0 to 20 years; thereafter it is held constant out to 1000 years. The reservoir is 4.75 to 5.0 km below the ground surface, with a geothermal heat flux of 75 mW/m², permeability = 1×10^{-13} m², bounded by seal units with permeability = 1×10^{-18} m²; all with 12 percent porosity and a thermal conductivity of 2.0 W/m °C. The extractors and CO₂ injectors are completed in the entire vertical extent of the reservoir and the brine injectors are completed in the upper half of the reservoir.

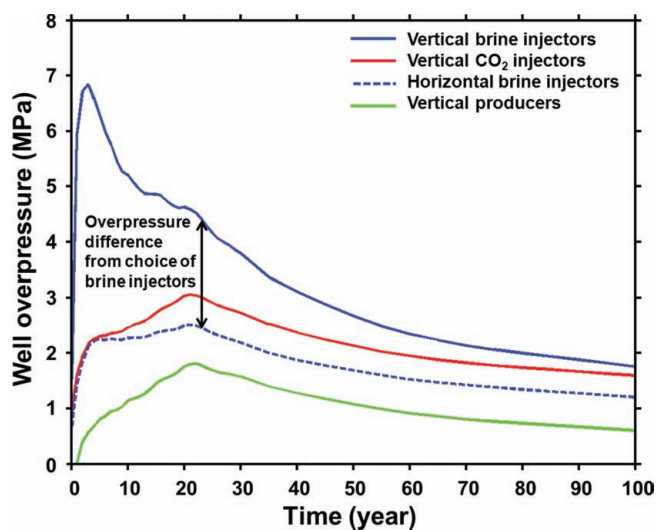


Figure 5. Overpressure history at the brine injectors, CO₂ injectors, and producers for the cases plotted in Figs 4 and 6 with a geothermal heat flux of 75 mW/m² and a reservoir bottom depth of 5 km. The vertical brine injectors pertain to Fig. 4 and the horizontal brine injectors pertain to Fig. 6. The difference in overpressure resulting from the choice of brine injector is shown.

is spread over a relatively wide area, thermal breakthrough has not yet occurred at 100 years (Fig. 4(d)), which will delay thermal drawdown, thereby extending the economic lifetime of this approach. However, had we considered permeability heterogeneity, fast pathways might have promoted earlier thermal breakthrough and drawdown.

To relieve overpressure at the brine injectors we considered a case where the outer ring of 8 brine injectors is replaced by four horizontal injectors (Fig. 6). While this change strongly reduces overpressure at the brine injectors (Fig. 5), it has little effect on the shape of the CO₂ plume (compare Fig. 6(b) with Fig. 4(b)) or on the shape of the thermal plume around the CO₂ injectors (compare Figs 6(c) and 6(d) with Figs 4(c) and 4(d)). The use of horizontal brine injectors can be a very effective means of spreading out the region of overpressure, thereby reducing the magnitude of overpressure. The pressure-support benefit of CO₂ injection on geothermal energy production is evident in Fig. 5. With the exception of very early time, the producers are always overpressured. Thus, pressure support from CO₂ injection reduces (or in this case, prevents) hydraulic drawdown at the geothermal producers, thereby reducing parasitic

pumping costs, which can be detrimental to the economics of geothermal operations.

Figure 7 and Table 3 summarize the fluid mass and heat extraction for the four temperature cases considered. Note that the extraction temperatures are bottom-hole temperatures and that wellhead temperatures will be significantly different when CO₂ is produced. Although CO₂ breakthrough occurs within 1 to 2 years, thermal conduction from the relatively large thermal footprint, compared to typical geothermal systems, slows further decline of extraction temperatures. Temperature decline during the first 100 years is small: 8.6, 7.8, 10.5, and 9.1 °C for the low, to high temperature cases, respectively, for a conservatively low CO₂ injection temperature of 16 °C (Table 3). For a more realistic (higher) CO₂ injection temperature that accounts for the Joule-Thomson effect, the temperature decline decreases only slightly (Table 3). Heat extraction rate is highest (434 to 1076 MWt) at early time when only brine is produced (Fig. 7(b)). The decline in heat extraction rate corresponds to CO₂ breakthrough and the continual increase in CO₂ cut (Fig. 7(a)), in addition to the fact that CO₂ carries less heat per unit mass than brine. Had we taken advantage of the lower viscosity of CO₂ (resulting in higher mobility) and the thermosyphon effect by increasing the fluid production rate, it may have been possible to maintain the heat extraction rate. Because the injected CO₂ plume is large (>50 km²), the heat extraction rate per unit area is small (9 to 22 MWt/km²), compared to the high rate (47 MWt/km²) in the 0.7071-km well spacing 5-spot case analyzed by Randolph and Saar (2011a),⁷ which explains why the three-ring well pattern resulted in a much slower rate of thermal drawdown.

Initially, because the CO₂ cut is equal to zero, the CO₂ delivery rate is equal to the CO₂ injection rate (480 kg/s or 15 MT/year). As the CO₂ cut increases (Fig. 7(a)), the CO₂ delivery rate becomes a smaller fraction of the injected CO₂, which increases the ratio of heat extraction per ton of delivered CO₂, while reducing the rate of increase of net (permanent) CO₂ storage (Fig. 7(c)). From a life-cycle analysis perspective, increasing the heat extraction per ton of delivered (i.e. captured) CO₂ is beneficial because it offsets a larger fraction of the parasitic energy cost associated with CO₂ capture. Conversely, carbon-intensity reduction increases with the amount of permanent CO₂ storage. Because the mobility ratio between CO₂ and brine decreases with increasing

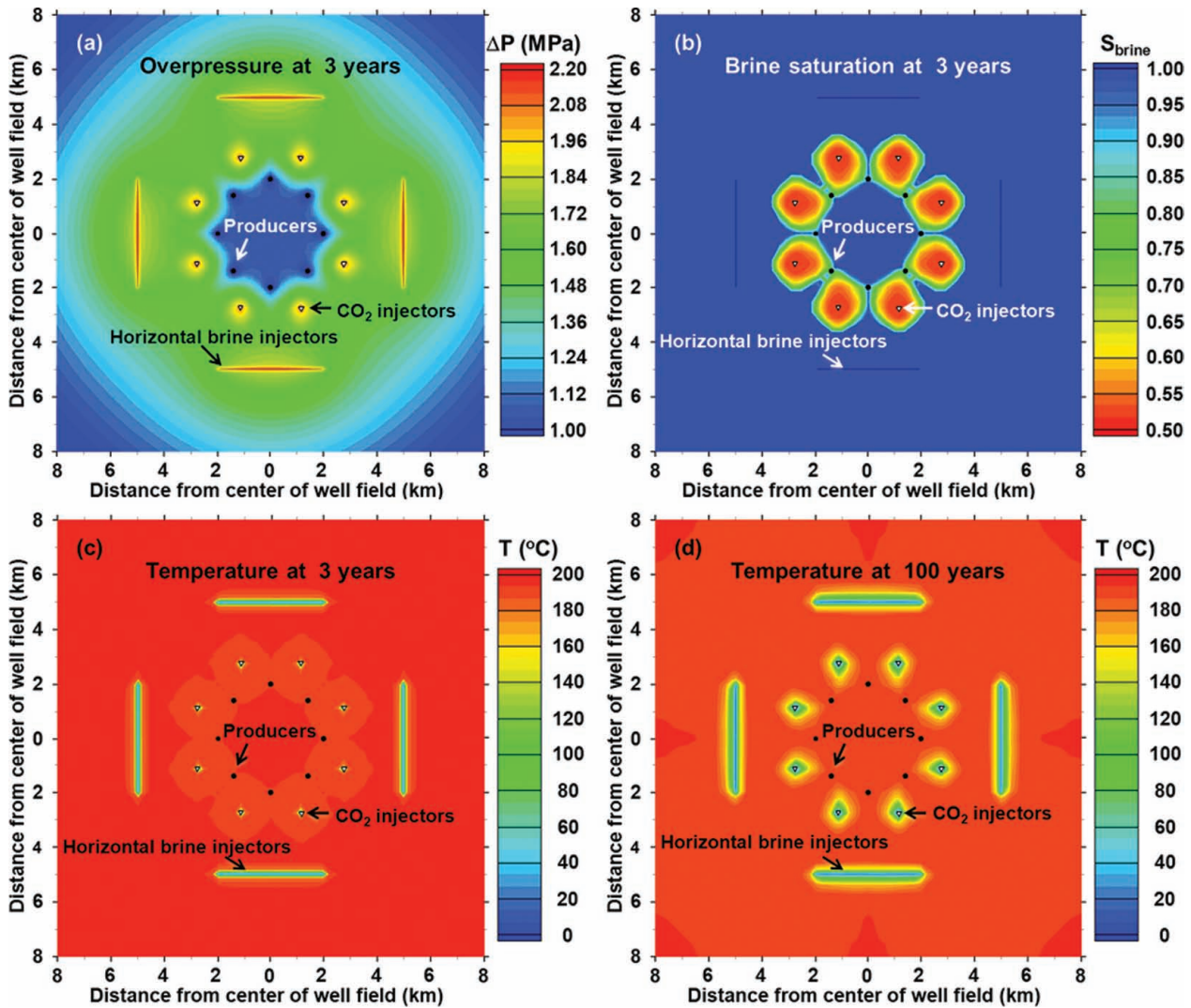


Figure 6. Overpressure, brine saturation, and temperature distributions are plotted at the indicated times for a symmetrical 24-spot, three-ring pattern of vertical and horizontal wells, including an inner ring of eight extractors (producers), 2 km from the center, a middle ring of 8 CO₂ injectors, 3 km from the center, and four brine injection wells, 5 km from the center. A fixed fluid extraction rate of 960 kg/s is maintained, while the CO₂ injection rate is ramped from 480 to 960 kg/s from 0 to 20 years; thereafter it is held constant out to 1000 years. The reservoir is 4.75 to 5.0 km below the ground surface, with a geothermal heat flux of 75 mW/m², permeability = 1×10^{-13} m², bounded by seal units with permeability = 1×10^{-18} m²; all with 12% porosity and a thermal conductivity of 2.0 W/m °C. The vertical wells are completed in the entire vertical extent of the reservoir and the horizontal brine injectors are located at the top of the reservoir.

temperature, the rate of increase of CO₂ cut decreases with increasing temperature (Fig. 7(a)). Thus, the low-temperature case requires less delivered CO₂ than the high-temperature case. Accordingly, the high-temperature case results in the greatest amount of permanent CO₂ storage (Fig. 7(c)). Note that had we considered permeability heterogeneity, fast

pathways would promote earlier CO₂ breakthrough, resulting in a more rapid increase in CO₂ cut and less permanent CO₂ storage. For our hybrid heat-extraction approach, brine is the predominant working fluid for early time, with the contribution of CO₂ to heat extraction increasing with CO₂ cut. The CO₂ heat extraction fraction reaches a value of 0.50 at

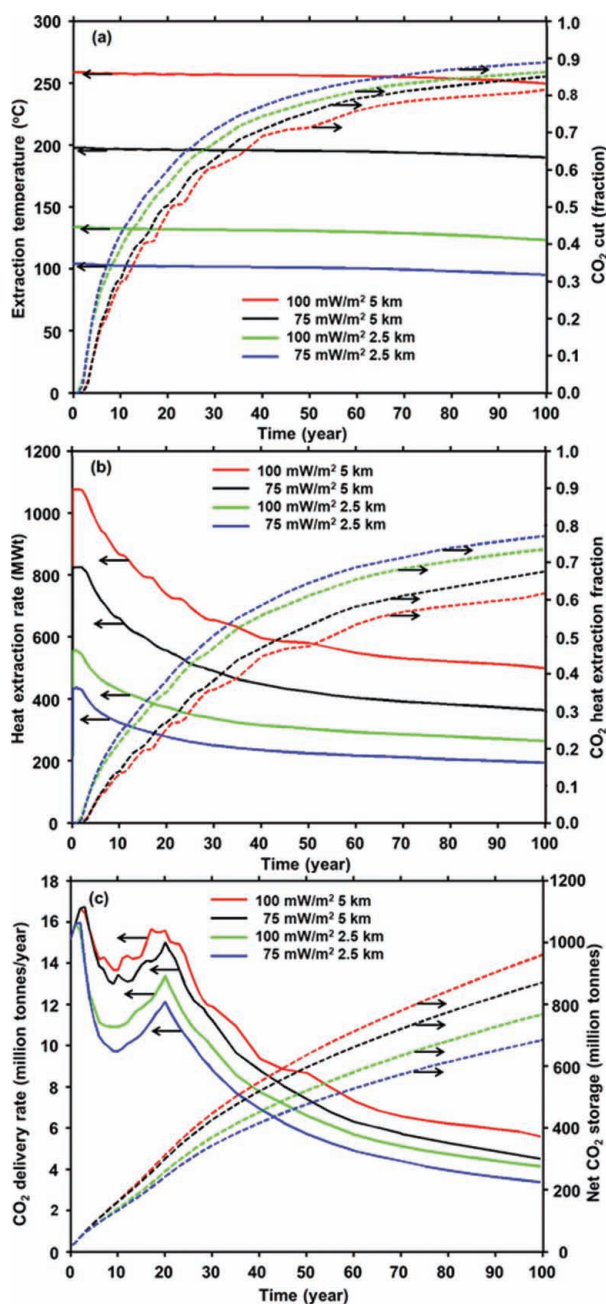


Figure 7. Histories of extraction temperature, CO₂ cut (fraction), heat extraction rate, and CO₂-storage are plotted for four cases using a symmetrical 24-spot, three-ring pattern of vertical wells, with geothermal heat fluxes of 75 and 100 mW/m², and for reservoir bottom depths of 2.5 and 5.0 km. CO₂ injection is ramped from 480 to 960 kg/s from 0 to 20 years; thereafter it is held constant out to 1000 years. Plots include (a) extraction temperature and CO₂ cut, (b) heat extraction rate (solid) and CO₂ heat extraction fraction (dash), and (c) CO₂ delivery rate (solid) and net CO₂ storage (dash). The CO₂ delivery rate is equal to the CO₂ injection rate minus the CO₂ extraction rate.

13.6, 15.8, 19.4, and 20.8 years (Fig. 7(b) and Table 3) for the low to high temperature cases, respectively; thereafter CO₂ would become the predominant working fluid. Note that the CO₂ injection temperature has no influence on the timing of CO₂ cut. Our results imply that it may be difficult to prevent either the co-production of brine for CO₂-based GEE, or the co-production of CO₂ for brine-based GEE (Fig. 7(a)). This finding reinforces the practicability of a staged GEE-GCS approach, where ACRM practice would be implemented throughout the second and third stages to minimize the risks associated with reservoir overpressure, and, where appropriate, to generate useful water resources.

Summary and conclusions

There are sites within the continental U.S. that would be suitable for integrating high-temperature GEE with GCS; however the prevalence of low-temperature sites makes it likely that widespread GEE-GCS deployment would include lower temperature sites. Our purpose herein was to demonstrate a possible utilization option for CO₂ capture, utilization and sequestration efforts occurring in the continental United States. We accomplished this by identifying potential sites within sedimentary formations where GEE-GCS can be implemented, using a staged approach to reduce operational exposure. Stage one involves re-circulating formation brine for reservoir characterization and geothermal energy production. Once characterization is sufficient to reduce operational exposure and to satisfy public acceptance, stage two can commence with CO₂ injection providing pressure support for the brine production wells. Stage three begins as CO₂ breaks through and is co-produced with brine, providing an additional working fluid; eventually CO₂ becomes the predominant working fluid for geothermal energy production. Model results of stages two and three of an GEE-GCS operation demonstrate how the use of a concentric three-ring well pattern developed in this paper shifts the region of maximum reservoir overpressure from the CO₂ injection wells (and CO₂ storage zone) out to the outer ring of brine reinjection wells, thereby suppressing CO₂ migration and leakage during active injection/extraction operations, and reducing the risk of brine migration away from the storage zone. Our analysis of a concentric extractor/injector/re-injector well pattern has shown longevity of thermal productivity from a suitable GEE

site, while providing sufficient CO₂ storage volume and trapping to act as a sequestration operation. Admittedly, there is low economic prospect of drilling the number of vertical wells required to fulfill this design. However, the advent of directional drilling, staged or sliding screens for well-casing perforations, and advanced reservoir management strategies could make this or a similar operation economically favorable. Future work will examine this aspect of ACRM GEE-GCS in the context of CO₂ as a pressure support and working fluid.

Acknowledgements

The authors would like to acknowledge funding support of the: US Department of Energy Grant DE-FE0000749, Natural Science and Engineering Research Council of Canada, and the Carbon Mitigation Initiative of Princeton University. This work was sponsored by USDOE Geothermal Technologies Program, by USDOE Fossil Energy, National Energy Technology Laboratory, by the Carbon Mitigation Initiative at Princeton University, and by the Environmental Protection Agency under Cooperative Agreement RD-83438501. This work was performed under the auspices of the U.S. Department of Energy by LLNL under contract DE-AC52-07NA27344.

References

1. Khashgi H, de Coninck H and Kessels J, Carbon dioxide capture and storage: Seven years after the IPCC special report. *Mitig Adapt Strategies Global Change* **17**(6):563–567 (2012).
2. Zhou Q, Birkholzer JT, Tsang C-F and Rutqvist J, A method for quick assessment of CO₂ storage capacity in closed and semi-closed saline formations. *Int J Greenhouse Gas Control* **2**:626–639 (2008).
3. Burton M, Kumar N and Bryant SL, Time-dependent injectivity during CO₂ storage in aquifers in *Soc Petrol Eng 113937 SPE/DOE Symposium on Improved Oil Recovery*, April 20–23, 2008, Tulsa, OK, USA (2008).
4. Yang G, Zhang Y and Li S-Q, Uncertainty analysis of carbon sequestration in an inclined deep saline reservoir. *AAPG Bulletin*, in press (2013).
5. Court B, Elliot TR, Dammel J, Buscheck TA, Rohmer J and Celia MA, Promising synergies to address water, sequestration, legal, and public acceptance issues associated with large-scale implementation of CO₂ sequestration. *Mitig Adapt Strategies Global Change* **17**(6):569–599 (2011).
6. Bandilla KW, Court B, Elliot TR and Celia MA, Comparison of brine production scenarios for geologic carbon sequestration operations in *OnePetro: Carbon Management Technology Conference*. DOI: 10.7122/151250-MS (2012).
7. Randolph JB and Saar MO, Coupling carbon dioxide sequestration with geothermal energy capture in naturally permeable, porous geologic formations: Implications for CO₂ sequestration. *Energy Procedia* **4**:2206–2213 (2011).
8. Buscheck TA, Active management of integrated geothermal-CO₂-storage reservoirs in sedimentary formations: An approach to improve energy recovery and mitigate risk, Proposal in response to DE_FOA-0000336: *Energy Production with Innovative Methods of Geothermal Heat Recovery*, LLNL-PROP-463758. (2010).
9. Buscheck TA, Sun Y, Hao Y, Wolery TJ, Bourcier WL, Tompson AFB *et al.*, Combining brine extraction, desalination, and residual-brine reinjection with CO₂ storage in saline formations: Implications for pressure management, capacity, and risk mitigation. *Energy Procedia* **4**:4283–4290 (2011).
10. Buscheck TA, Sun Y, Chen M, Hao Y, Wolery TJ, Bourcier WL *et al.*, Active CO₂ reservoir management for carbon storage: Analysis of operational strategies to relieve pressure buildup and improve injectivity. *Int J Greenhouse Gas Control* **6**:230–245 (2012).
11. Pruess K, Enhanced geothermal systems (EGS) using CO₂ as working fluid – a novel approach for generating renewable energy with simultaneous sequestration of carbon. *Geothermics* **35**:351–367 (2006).
12. Randolph JB and Saar MO, Impact of reservoir permeability on the choice of subsurface geothermal heat exchange fluid: CO₂ versus water and native brine. *Proceedings for the Geothermal Resources Council 35th Annual Meeting*, 23–26 October, San Diego, CA, USA (2011).
13. Saar MO, Randolph JB and Kuehn TH, *Carbon Dioxide-based geothermal energy generation systems and methods related thereto*. US Patent 20120001429 (2010).
14. Chapuis F, Bauer H, Grataloup S, Leynet A, Bourguin B, Castagnac C *et al.*, Geological investigations for CO₂ storage: From seismic and well data to 3D modeling, *Energy Procedia* **4**:4591–4598 (2011).
15. Stephens JC and Justo S, Assessing innovation in emerging energy technologies: Socio-technical dynamics of carbon capture and storage (CCS) and enhanced geothermal systems (EGS) in the USA. *Energy Policy* **38**:2020–2031 (2010).
16. Nordbotten JM and Celia MA, An improved analytic solution for interface upconing around a well. *Water Resour Res* **42**:W08433 (2006).
17. Mantilla CA, Srinivasan S, Cross EA and Brant SL, Inexpensive assessment of plume migration during CO₂ sequestration. *Soc Petrol Eng* 126693 (2009).
18. Michael K, Arnot M, Cook P, Ennis-King J, Funnell R, Kaldi J *et al.*, CO₂ storage in saline aquifers I – Current state of knowledge. *Energy Procedia* **1**:3197–3204 (2009).
19. Celia MA, Nordbotten JM, Court B, Dobossy M and Bachu S, Field-scale application of a semi-analytical model for estimation of CO₂ and brine leakage along old wells. *Int J Greenhouse Gas Control* **5**(2):257–269 (2011).
20. Nitao JJ, *Reference manual for the NUFT flow and transport code, version 3.0*. Lawrence Livermore National Laboratory. UCRL-MA-130651-REV-1, (1998).
21. Carr TR, Rich PM and Bartley JD, The NATCARB geoportal: Linking distributed data from the carbon sequestration regional partnerships. *J Map Geogr Libr* **4**:131–147 (2007).
22. Mooney WD and Kaban MK, The North American upper mantle: Density, composition, and evolution. *J Geophys Res* **115**:1–24 (2010).

23. Blackwell DD and Richards M, *Geothermal Map of North America*. American Association of Petroleum Geologists (AAPG), 1 sheet, scale 1:6,500,000 (2004).
24. Blackwell DD, Negraru P and Richards M, Assessment of the enhanced geothermal system resource base of the United States. *Nat Res Research* DOI: 10:1007/s11053-007-9028-7 (2007).
25. Wan Z, New refinements and validation of the MODIS land-surface temperature/emissivity products. *Remote Sens Environ* **112**:59–74 (2008).
26. Nordbotten JM, Celia MA, Bachu S and Dahle HK, Semianalytical solution for CO₂ leakage through an abandoned well. *Environ Sci Technol* **39**(2):602–611 (2005).
27. Chadwick J, *Depositional environments, diagenesis, and porosity/permeability relationships of the Ellenburger group in the Pegasus field Midland/Upton County, Texas*, master of science thesis. Texas Tech University (1987).
28. Railroad Commission of Texas, Oil and Gas Records. [Online]. Available at: <http://www.rrc.state.tx.us/data/wells/wellrecords.php> [July 1, 2012].
29. Nogue JP, Court B, Dobossy M, Nordbotten JM and Celia MA, A methodology to estimate maximum probable leakage along old wells in a geologic sequestration operation. *Int J Greenhouse Gas Control* **7**:39–47 (2012).
30. Zhou Q, Birkholzer JT, Tsang C-F and Rutqvist JA, A method for quick assessment of CO₂ storage capacity in closed and semi-closed saline formations. *Int J Greenhouse Gas Control* **2**:626–639 (2008).
31. Buscheck TA, Sun Y, Hao Y, Chen M, Court B, Celia MA and Wolery TJ, Geothermal energy production from actively-managed CO₂ storage in saline formations, *Proceedings for the Geothermal Resources Council 35th Annual Meeting*. 23–26 October 2011, San Diego, CA, USA, (2011b).
32. Buscheck TA, Elliot TR, Celia MA, Chen M, Hao Y, Lu C and Sun Y, Integrated, geothermal-CO₂ storage reservoirs: adaptable, multi-stage, sustainable, energy-recovery strategies that reduce carbon intensity and environmental risk, *Proceedings for the Geothermal Resources Council 36th Annual Meeting*. September 30–October 3, Reno, NV, USA (2012).
33. ASME. *ASME Steam Tables Compact Edition*. ASME, Three Park Avenue, New York, NY (2006).
34. Span R and Wagner W, A new equation of state for carbon dioxide covering the fluid region from the triple-point temperature to 1100K at pressures up to 800 MPa. *J Phys Chem Ref Data* **25**:1509–1596 (1996).
35. Fenghour A, Wakeham WA and Vesovic V, The viscosity of carbon dioxide. *J Phys Chem Ref Data* **27**(1):31–44 (1998).
36. Bourcier WL, Wolery TJ, Wolfe T, Haussmann C, Buscheck TA and Aines RD, A preliminary cost and engineering estimate for desalinating produced formation water associated with carbon dioxide capture and storage. *Int J Greenhouse Gas Control* **5**:1319–1328 (2011).
37. Spycher N and Pruess K, A model for thermophysical properties of CO₂-brine mixtures at elevated temperatures and pressures. *Proceedings for the 36th Stanford Geothermal Workshop*. 31 January–2 February, Stanford University, Palo Alto, CA (2010).
38. Katz DL and Lee RL, Physical behavior of natural gas systems physical and thermal properties, phase behavior, analyses, in *Natural Gas Engineering*. McGraw-Hill Publishing Company, New York, NY, pp. 110–196 (1990).
39. Zobac MD and Gorelick SM, Earthquake triggering and large-scale geologic storage of carbon dioxide, *P Natl Acad Sci* **109**(26):10164–10168 (2012).
40. Brown DW, A hot dry rock geothermal energy concept using supercritical CO₂ instead of water. *Proceedings of the Twenty-Fifth Workshop on Geothermal Reservoir Engineering*. Stanford University, pp. 233–238 (2000).
41. Randolph JB and Saar MO, Combining geothermal energy capture with geologic carbon dioxide sequestration. *Geophys Res Lett* **38**:L10401 (2011).



Tom Elliot

Tom Elliot has focused on the use of subsurface resources from an earth, hydrologic and energy perspective. Ongoing research projects include the co-localization of resource utilization schemes to realize synergistic operation; influence of thermal stress on subsurface operations; suitable model complexity for simulation of large scale two-phase flow at depth; and methods of simulating the subsurface environment using numerical coupling of processes. His studies rely on a cooperative relationship with industry partners, as well as a multidisciplinary research collaboration that includes government, university and private research organizations.



Thomas Buscheck

Thomas Buscheck is group leader of Geochemical, Hydrological, and Environmental Sciences at Lawrence Livermore National Laboratory. He received his BSc from Lafayette College and his MSc and PhD from the University of California at Berkeley, all in Civil Engineering. His research interests involve multiphase heat and mass flow in porous media, with applications to geologic radioactive waste isolation, geologic CO₂ storage, hydrocarbon recovery, and geothermal energy.



Michael Celia

Michael Celia is the Theodora Shelton Pitney Professor of Civil and Environmental Engineering at Princeton University. He received his BSc from Lafayette College and his MSc and PhD from Princeton University. His research interests include groundwater hydrology, multiphase flow in porous media and numerical simulation methods, with applications to subsurface transport processes and subsurface technologies associated with climate-change mitigation and global sustainability.